

RESEARCH ARTICLE

Vertical Seismic Action for Design: Developments for the Next Generation of European and Italian Norms

Chiara Smerzini¹  | Roberto Paolucci¹  | Sara Sgobba²  | Fadel Ramadan² 

¹Department of Civil and Environmental Engineering, Politecnico Di Milano, Milano, Italy | ²Istituto Nazionale di Geofisica e Vulcanologia (INGV), Sezione Milano, Italy

Correspondence: Chiara Smerzini (chiara.smerzini@polimi.it)

Received: 19 May 2025 | **Revised:** 10 September 2025 | **Accepted:** 27 October 2025

Keywords: Eurocode 8 | probabilistic seismic hazard assessment | seismic norms | vertical response spectrum | vertical-to-horizontal spectral ratios

ABSTRACT

This paper addresses the definition of the vertical seismic action for design, within the progress studies for the next generation of the European and Italian seismic norms, partly still in progress. Besides presenting the background of the vertical design spectra according to the second generation of the Eurocode 8, a period-dependent factor for the Vertical-to-Horizontal (V/H) response spectral ratios is introduced, following the findings from recent empirical studies. The proposed V/H factor is expressed in a simple format as a function of relatively few parameters (i.e., seismicity level and site conditions), which are typically adopted in a normative framework, being, at the same time, suitable to identify the main physical factors affecting the V/H ratios. This factor is found to explain reasonably well the results of probabilistic seismic hazard analyses for both H and V components conducted for selected test sites in Italy, with different approaches to account for the V component. A favorable comparison with probabilistic results is also obtained for the V/H spectral ratios according to the new Eurocode 8.

1 | Introduction

It was 1916 when, to guide the reconstruction after the catastrophic earthquakes of the Messina Straits (Southern Italy, 1908) and of Southern Abruzzi (Central Italy, 1915), the Italian norms first prescribed quantitatively the seismic forces to be applied to structures as a percentage of their weight. Similar regulations were later introduced in Japan after the Great Kanto earthquake in 1923, and in the United States, after the 1933 Long Beach earthquake.

In the 1916 norms, the horizontal forces were prescribed to be 1/8 and 1/6 of the weight at the first floor and subsequent floors, respectively, while, for the vertical force, the weight of the structure was increased by 50%. Therefore, the vertical component of motion was considered to be by far larger than the horizontal one. Although seismometry had already been

developed by that time, especially in Japan and Italy [1], the first instruments did not provide detailed information on ground accelerations and no near-source record was yet available [2, 3]. Owing to the understanding that seismic waves originated by the seismic source were predominantly longitudinal, it was believed that the ground motion in the proximity of the epicenter was prevalently vertical (*moto sussultorio* in Italian), while the horizontal components (*moto ondulatorio*) were expected to become prevailing at larger distances from the epicenter (Ravà et al. 1906, quoted by Penta [4]). Still, in one of the first introductory texts of Earthquake Engineering [5], where the pioneering concept of what was later referred to as the elastic response spectrum [6, 7] was first introduced, the attention was focused on the effects of the horizontal components of earthquake ground motion on structures, because it was argued that the vertical one was not of concern for well-connected structural systems.

As more strong motion records became available, Newmark and Hall [8] introduced, in their seminal textbook, the 2/3 scaling factor to obtain the vertical (V) spectrum from the horizontal (H) one, as a rule-of-thumb to represent the observations from the earthquake ground motions recorded at that time. They further justified the standard assumption of neglecting the relevance of V accelerations in design both by the high factors of safety commonly inherent to the building design under gravity loads and by the fact that V components may be significantly out-of-phase with the H ones. Indeed, Ambraseys and Douglas [9] observed that the ratio of the V spectral response that occurs at the time of the maximum H response, for the same period T , does not exceed 0.2 and is insensitive to magnitude and distance. Note that, according to the building code currently in force in the United States, ASCE 7–22 [10], the seismic load effects on the V component are proportional to 20% of the design spectral response acceleration at short periods. The 0.2 factor is the result of the 100%–30% combination rule proposed by Rosenblueth and Contreras [11], with the rule-of-thumb $V/H = 2/3$, but it can also be viewed in agreement with the findings by Ambraseys and Douglas [9].

Most norms for seismic design require specific consideration of the vertical seismic action only for a relatively limited set of structures or structural elements that are sensitive to V accelerations, such as horizontal cantilevers, long-span structural members, base-isolated systems, bridge elements, vertically-sensitive industrial structures and equipment such as tanks and vessels [10, 12]. For geotechnical structures the V component is typically considered for slope stability analyses, for which, in case of pseudo-static verifications, the V acceleration is often considered as one-half of the H one, acting in both upward and downward directions (see e.g., Eurocodes 8 Part 5 [13]). Furthermore, the consideration of the V component for design is often enforced upon the exceedance of prescribed threshold values of the seismic action.

Recent empirical studies have pointed out some distinctive features of the V component of ground shaking, compared to the H one, in terms of spectral content, attenuation rate and site response [14–21], such as:

- V motion may be richer at higher frequencies (shorter periods of vibration) than the H one, and such difference is more pronounced at soft sites and at short distances from the earthquake source;
- the attenuation rate with distance of V motion is faster, owing to hysteretic damping that is more effective at high frequencies;
- site response effects, including non-linear behavior at large soil strains (e.g., in the near-field region), are more significant on the H component than on the V motion.

As discussed in further detail in the following, such observational evidences have been incorporated in recent international seismic norms with different levels of detail and complexity: from the simplest prescriptions of the 2024 New Zealand Standards [22], where a constant V/H is assumed, regardless of site conditions, up to the more detailed ASCE standards [23], where a refined, period-dependent V/H spectrum is defined as a function of the seismicity level and site conditions.

In the frame of such international normative context and, in particular, of the studies for the next generation of the European [24] and Italian seismic norms, still in progress in the second case, the main objective of this paper is to introduce a simplified parametrization of the V/H response spectral ratios as a function of relatively few hazard parameters (such as the peak ground acceleration or site response proxies) and to assess its performance in comparison with different code-based formulations. For this purpose, a period-dependent V/H factor is proposed on the basis of the findings from a recent empirical study on the V/H ratios from earthquake strong motions recorded in Italy. Such factor is formulated in a format suitable to investigate easily how the seismicity level, the source-to-site distance, and site effects may affect the V/H ratio, in support to the definition of the V seismic action in a normative context. Furthermore, the performance of such simplified V/H factor is discussed, together with other code-based ratios such as the ones recently issued in the Part 1 of the Eurocode 8 of second generation [12], with respect to the Uniform Hazard Spectra (UHS) obtained from Probabilistic Seismic Hazard Assessment (PSHA) studies. To this end, a simplified PSHA is performed at selected Italian sites, representative of various seismicity levels, considering, on one side, a separate PSHA for both the H and V components and, on the other side, the H component alone, with the V spectrum derived from a Ground Motion Model (GMM) for the V/H ratio, with magnitude and distance obtained by disaggregation of the H hazard.

The paper is organized as follows. After presenting an overview of the V seismic action according to different international standards, with emphasis on the design spectra defined in the Eurocode 8 of second generation, our proposal for the V/H factor is presented and discussed in detail, in relation to the main findings from empirical studies. Then, the paper focuses on the hazard consistency of the proposed factor by considering different approaches to derive the V response spectra based on the PSHA results.

2 | Overview of V/H Spectral Ratios From International Seismic Norms

As anticipated in the Introduction, different international standards have incorporated an elastic spectrum for the V component with different levels of detail: from the simplest prescriptions of the 2024 New Zealand Standards DZ TS 1170.5:2024 [22], where a constant $V/H = 0.7$ is assumed for source-to-site distance larger than 10 km, and $= 1$ for shorter distance, regardless of site conditions, up to the more detailed ASCE 7–22 standards [10]. In the latter case, to obtain the V design spectrum for structures sensitive to vertical motions, the H spectrum is multiplied by a period-dependent V/H spectral ratio, mainly inspired by the studies by Bozorgnia and Campbell [14]. Such design V/H ratio has the following main features (Figure 1):

- the short-period portion is controlled by the parameter C_v , which depends both on site conditions (i.e., V_{S30} , average shear wave velocity in the top 30 m) and on the level of seismic demand, with values typically ranging from 0.7 (low seismicity) to 1.5 (high seismicity, soft soils);

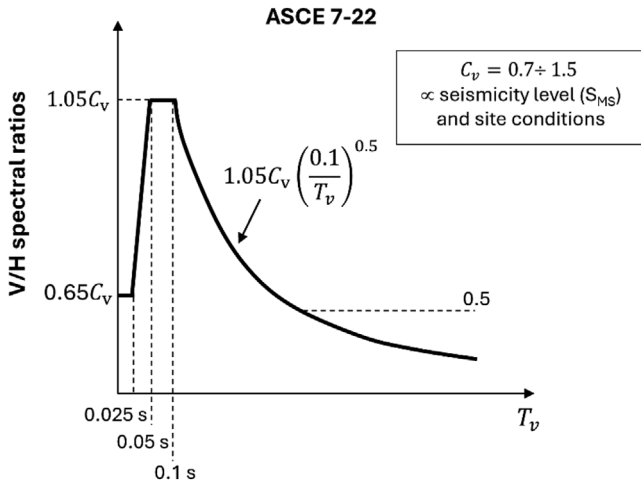


FIGURE 1 | Formulation of the V/H spectral ratios according to ASCE 7-22, following NEHRP [26]. The V/H ratios are referred to the geometric mean horizontal spectral ordinate (i.e., the F_{md} conversion factor to convert to a maximum direction spectral ordinate is neglected herein). The values of C_v range from 0.7 to 1.5 depending on the seismicity level and site conditions. Adapted from Figure C11.9-2 of ASCE 7-22.

- the intermediate part decays as a function of period as $T^{-0.50}$ (note that, in the previous version of U.S. provisions, ASCE 7-16 [25], such decay was faster, as $T^{-0.75}$);
- at periods larger than about 0.3–0.5 s, the V/H ratio tends to saturate to a constant value which is taken equal to 0.5.

Figure 2 shows a comparison of the code-based V/H spectral ratios according to different international standards, namely: the new generation of Eurocode 8, hereafter referred to as EC8-1-1 [12], the Italian Building Code NTC18 [27], ASCE 7-22, the Turkish Building Earthquake Code TBEC18 [28], the New Zealand norm DZ TS 1170.5:2024, and the new version of the Indian seismic code CED 39/T-10 [29]. For this comparison, the spectral parameters have been defined to ensure consistent elastic design spectra corresponding to a high seismicity site on both generic rock (left) and soft (right) site conditions, with base hazard parameters and site categories, for each seismic norm, as specified in the legend. Considering that full consistency among the different design spectra and site conditions cannot be achieved, an overall satisfactory agreement is found among the V/H ratios for the various seismic norms for both rock and soft soil: all the norms considered provide peak values of the V/H ratios in the short period range, at periods less than 0.1 s, and converge mostly to values around 0.6, on average, at long periods. The dependence of the V/H ratios on site conditions is generally taken into account by the seismic norms, in an explicit (e.g., ASCE 7-22) or implicit way (e.g., EC8-1-1), except for the New Zealand seismic code, with a slight-to-moderate effect.

2.1 | Elastic Vertical Response Spectrum in the Eurocode 8 of Second Generation

In the EC8-1-1, the H elastic spectrum for design is defined by a regularized functional form, defined as a function of two

parameters, $S_{\alpha,RP}$ and $S_{\beta,RP}$, corresponding to the constant acceleration branch and to the 1 s (T_β) spectral ordinate, respectively, for different return periods (RP). Although values of $S_{\alpha,RP}$ and $S_{\beta,RP}$ shall be provided by the National Annexes of the member Countries, the informative Annex A of EC8-1-1 presents maps of $S_{\alpha,475}$ and $S_{\beta,475}$ for the RP of 475 years obtained from the 2020 European Seismic Hazard Model ESHM20 [30]. According to the site categorization and the calculation of the site amplification factors F_α and F_β [31], the spectral ordinates $S_\alpha = F_\alpha S_{\alpha,RP}$ and $S_\beta = F_\beta S_{\beta,RP}$ are then obtained (aside from a topography amplification factor F_T that will not be considered hereafter).

Once S_α and S_β have been defined, the expression of the elastic 5% damped H response spectrum in the EC8-1-1 is obtained by the following equations:

$$0 \leq T \leq T_A : S_e(T) = \frac{S_\alpha}{F_A} \quad (1)$$

$$T_A < T \leq T_B : S_e(T) = \frac{S_\alpha}{T_B - T_A} \left[(T - T_A) + \frac{T_B - T}{F_A} \right] \quad (2)$$

$$T_B < T \leq T_C : S_e(T) = S_\alpha \quad (3)$$

$$T_C < T \leq T_D : S_e(T) = \frac{S_\beta T_\beta}{T} \quad (4)$$

$$T > T_D : S_e(T) = T_D \frac{S_\beta T_\beta}{T^2} \quad (5)$$

where values of the corner periods T_A , T_B , T_C , and T_D , and of F_A should be defined by the different member countries as Nationally Determined Parameters (NDP), with standard reference values introduced in EC8-1-1. In the equations above, $T_\beta = 1$ s.

The V component of the seismic action is obtained by the same functional form as the H spectrum, defined by Equations (1)–(5), where the parameters S_α , S_β , T_B , and T_C are replaced by their V counterparts, namely $S_{\alpha v}$, $S_{\beta v}$, T_{Bv} , and T_{Cv} , as given by Equations (6)–(9):

$$S_{\alpha v} = f_{vh\alpha} S_\alpha \quad (6)$$

$$S_{\beta v} = f_{vh\beta} S_\beta \quad (7)$$

$$T_{Cv} = \left[\frac{S_{\beta v} T_\beta}{S_{\alpha v}} \right] \quad (8)$$

$$T_{Bv} = 0.05 \text{ s} \quad (9)$$

where

$$f_{vh\alpha} = \begin{cases} 0.6 & \text{if } S_\alpha < 2.5 \text{ m/s}^2 \\ 0.04S_\alpha + 0.5 & \text{if } 2.5 \text{ m/s}^2 \leq S_\alpha \leq 7.5 \text{ m/s}^2 \\ 0.8 & \text{if } S_\alpha > 7.5 \text{ m/s}^2 \end{cases} \quad (10)$$

and

$$f_{vh\beta} = 0.6 \quad (11)$$

are the parameters representing the V/H response spectral ratio at short periods and at $T_\beta = 1$ s.

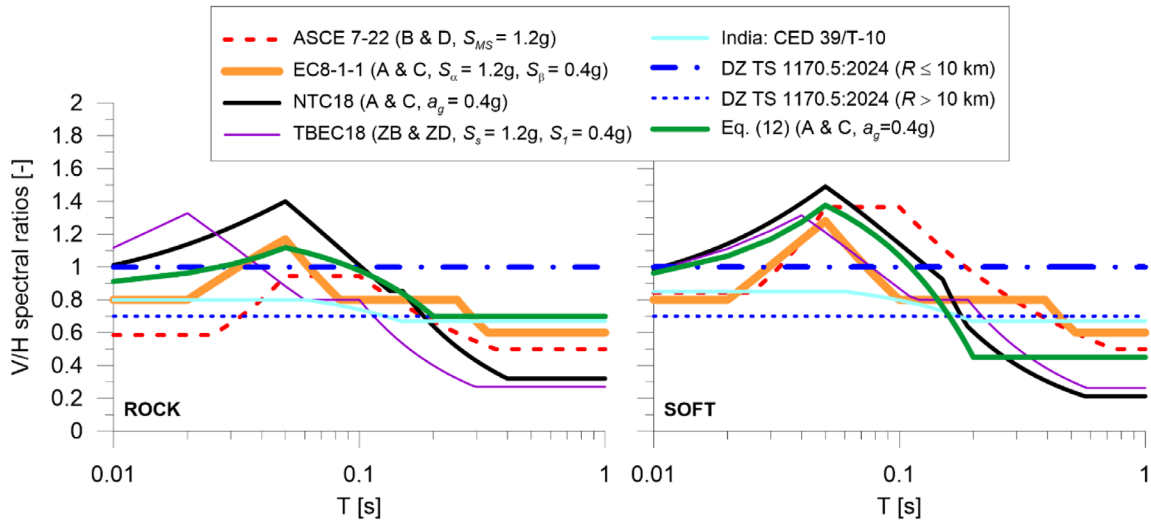


FIGURE 2 | Overview of code-based V/H ratios according to different international seismic codes for generic rock (left) and soft soil conditions (right). The base hazard parameters and site classes considered for each seismic norm are specified in the legend entries (S_{MS} : risk-targeted maximum considered earthquake spectral response acceleration at short periods according to ASCE 7–22; S_{α} and S_{β} : short and 1 s spectral response acceleration according to EC8-1-1; S_s and S_l : short and 1 s spectral response acceleration according to TBEC18; a_g : peak ground acceleration; R : source-to-site distance).

The rationale behind Equations (6)–(11) is to provide a simple expression for the V spectrum consistent with the same regularized shape as the H spectrum, where the short and intermediate spectral parameters ($f_{vh\alpha}$ and $f_{vh\beta}$, respectively) and the corner period T_{Bv} are tuned in a way to approach, albeit in a simplified way, the observational findings introduced in the subsequent section. Namely, the intermediate factor $f_{vh\beta}$ is equal to 0.6, independent of the seismicity of the area and of the site conditions, while $f_{vh\alpha}$ varies from low seismicity, where it is 0.6, thus reproducing a constant $V/H = 0.6$ for all periods, to high seismicity, where it attains a maximum value of 0.8. Furthermore, again for sake of simplicity, $T_{Bv} = 0.05$ s. Therefore, the V/H dependency on the period T and on site conditions is not explicitly stated, as in the ASCE 7–22, but it is made implicit by the dependence of $S_{\alpha v}$ and $S_{\beta v}$ in Equations (6) and (7) on the H spectral parameters S_{α} and S_{β} through the factors $f_{vh\alpha}$, $f_{vh\beta}$ and T_{Bv} . The V/H dependence on period from EC8-1-1 is compared to the other international standards in Figure 2.

As an illustrative example, Figure 3 shows the comparison of H and V elastic design spectra at 5% damping according to EC8-1-1 on reference outcropping rock conditions for both a high seismicity (left) and low seismicity (right) ideal site. In the bottom panel of this figure, pseudo-acceleration (PSA), pseudo-velocity (PSV), and spectral displacements (D) of the EC8-1-1 design spectra are illustrated using the well-known tripartite format.

3 | V/H Ratios: Empirical Findings and Proposal of a Simple Hazard-Related Factor

This Section aims at proposing a simple formulation for the V/H ratios, having the twofold objective, on one side, to identify the main trends of the V/H variability with magnitude, source-to-site distance and site conditions, on the basis of recent empirical evidences, and, on the other side, to be parametrized in terms of relatively few parameters in a format suitable to be potentially

cast in a normative framework. For this purpose, after recalling the main features of a recent empirical GMM based on Italian records, which form the majority of strong motion recordings in Europe, the proposed function and parameters for the V/H factor are described in detail.

3.1 | Findings from Recent Empirical Studies

To scrutinize the behavior of the V/H response spectral ratios as a function of some basic explanatory variables, such as vibration period, earthquake magnitude, source-to-site distance and site conditions, the GMM recently proposed by Ramadan et al. [21] and calibrated on the records from Italian crustal earthquakes, referred to hereafter as ITA18 -NESS, is considered. This GMM for the V/H ratios is fully consistent with ITA18, the GMM developed by Lanzano et al. [32] for the H components, that is the most updated reference for Italy, providing predictions of Peak Ground Acceleration (PGA), Peak Ground Velocity (PGV), and 5% damped spectral accelerations (PSA) over periods ranging from 0.01 to 10 s. The ITA18 -NESS V/H model further incorporates an adjustment factor, to account for near-source effects using the NESS (NEar-Source Strong-motion) flat-file [33, 34]. The latter is a global dataset of near-source ground motion recordings designed to capture source-related effects that are typically under-represented in broader datasets like ITA18. As explained in Ramadan et al. [21], the calibration of the ITA18-NESS GMM required a high-quality manual processing of the records, with consistent low-pass filtering frequencies for the H and V components of ground motion, according to the procedure by Paolucci et al. [35]. Note that this empirical model for the V/H ratios serves as a basis for the parametrization and calibration of the proposed V/H factor, as explained in detail in the following section, in a simpler form than the one used in standard GMM.

Figure 4 shows a set of median V/H ratios from the ITA18-NESS GMM for different values of moment magnitude (M_w), Joyner-

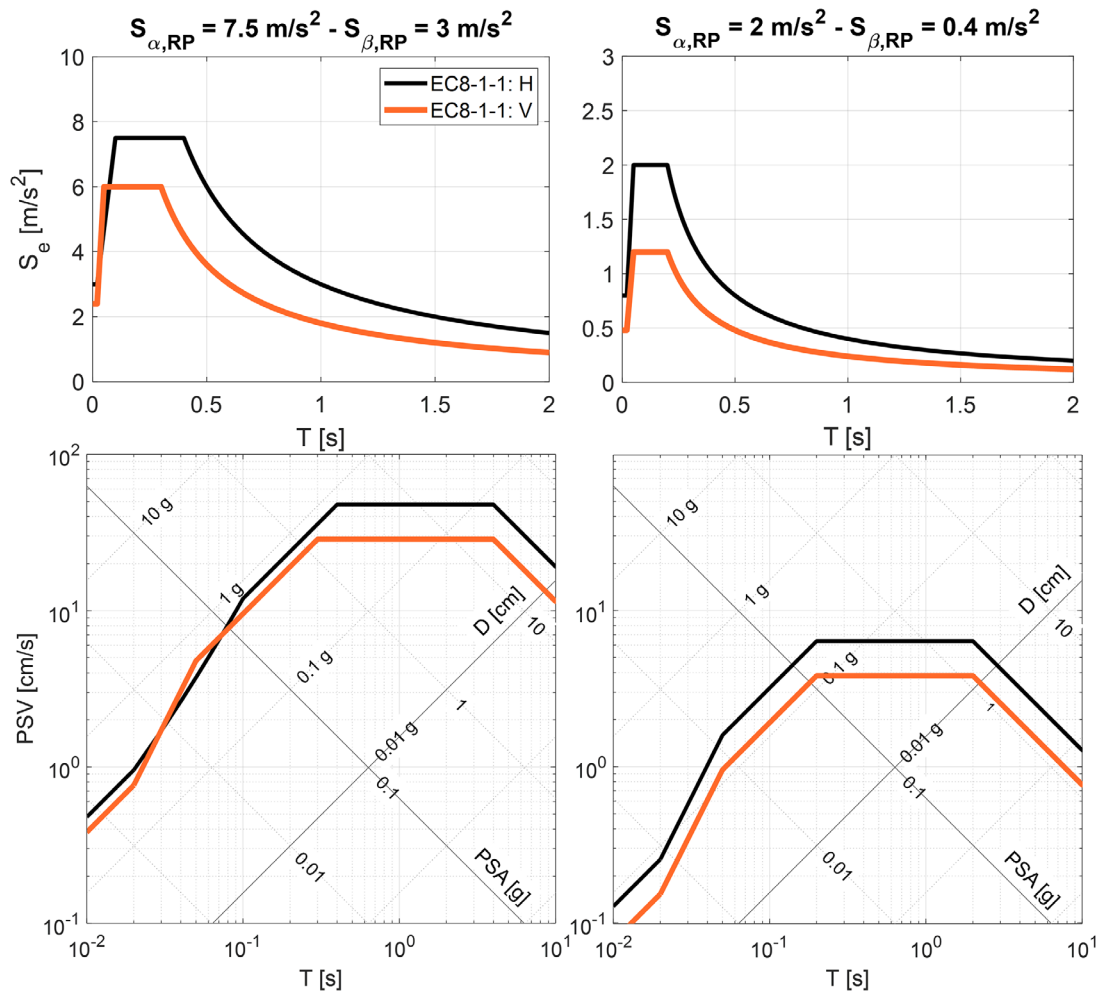


FIGURE 3 | Comparison of H and V elastic design spectra according to EC8-1-1 on reference outcropping rock conditions for both a high seismicity (left: $S_{\alpha,RP} = 7.5 \text{ m/s}^2$, $S_{\beta,RP} = 3 \text{ m/s}^2$) and low seismicity (right: $S_{\alpha,RP} = 2.0 \text{ m/s}^2$, $S_{\beta,RP} = 0.4 \text{ m/s}^2$) ideal site. The bottom panel shows the design spectra using the tripartite format (PSA: pseudo-acceleration; PSV: pseudo-velocity; D: spectral displacement).

Boore distance R_{JB} (referred to as R hereafter) and soil conditions (in terms of V_{S30}), namely: $M_W = 5.0$ (left panel), 6.0 (center) and 7.0 (right); $R = 5, 15$ and 30 km ; $V_{S30} = 150 \text{ m/s}$; 270 m/s and 560 m/s . The average of the median V/H for the different focal mechanisms (NF = Normal Fault; TF = Thrust Fault; SS = Strike-Slip) is considered herein and in all analyses discussed in the following sections, because of the limited dependence of the V/H ratios on the style of faulting, as found by Ramadan et al. [21]. In line with other empirical studies based on worldwide datasets [15, 17, 36–38], the trends of Figure 4 point out the following distinctive features of the V/H ratios:

- at $T = 0$ (PGA), V/H lies typically within the range between about 0.5 and 0.8, with larger values for increasing magnitude and decreasing distances, thus suggesting a correlation with the seismicity of the site;
- correlation with site conditions is reflected by larger V/H values at short periods (between 0.05 and 0.1 s) and smaller values at longer periods (beyond 0.3 s), as V_{S30} decreases; however, these effects are significant only for very soft soils;
- V/H shows a distinct peak at very short periods, typically between 0.05 and 0.07 s, with values that may exceed unity

in the near-source region of large magnitude events. While the peak period is approximately constant, regardless of M_W , R and of site conditions, the peak amplitude is clearly affected by site conditions. In line with previous studies [14, 15], the peak of V/H tends to exceed unity for soil sites at closer distance from the source and larger magnitudes, probably due to the different impact of non-linear site effects that tend to impact more the H motion (mostly related to shear strains of deviatoric nature) than the V one.

- for periods longer than about 0.3–0.5 s, V/H tends to be bounded within a relatively narrow range of values, with an increasing trend with V_{S30} , from about 0.3 to 0.75.

The variability of the V/H ratios with respect to that of the H and V GMM, relevant, for instance, for those approaches aimed at deriving the vertical Conditional Mean Spectrum [38], are discussed thoroughly in Ramadan et al. [21].

3.2 | Proposed V/H Factor

Aiming at making a synthesis of the previous empirical studies in a simple format suitable to highlight the main physical factors

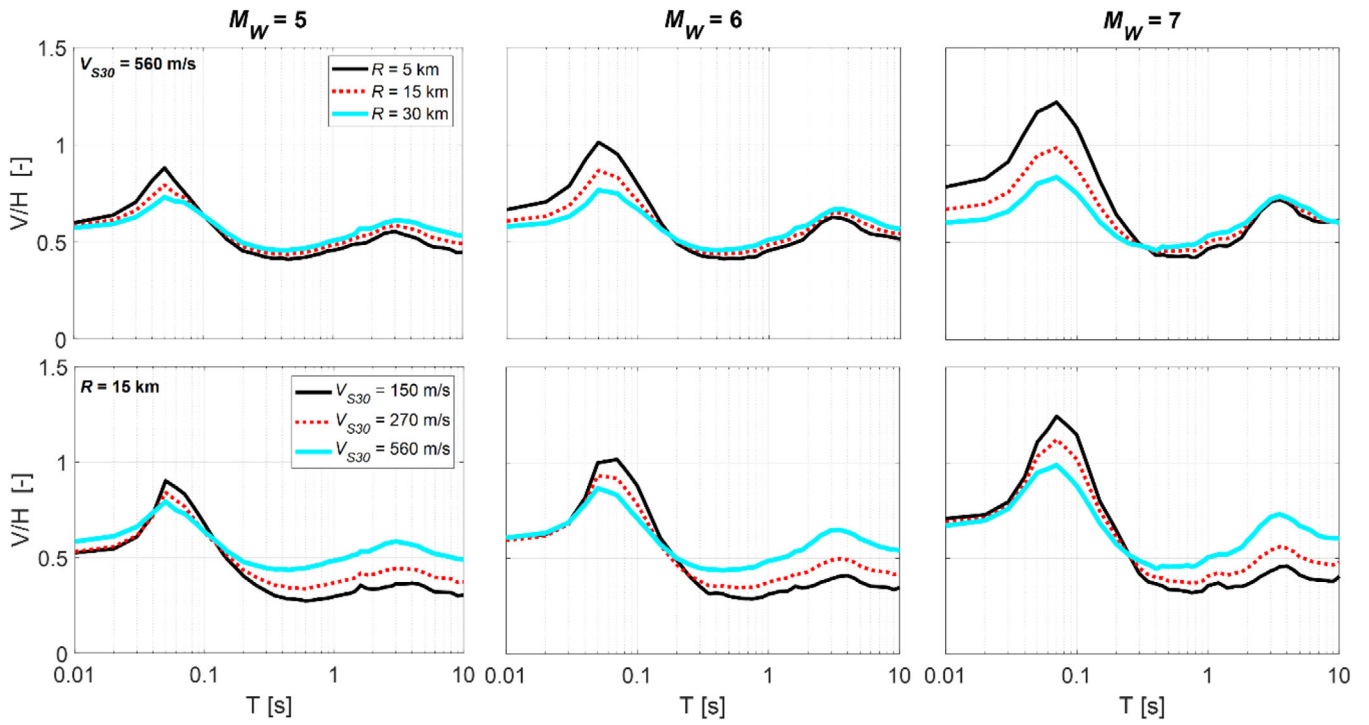


FIGURE 4 | Median V/H response spectral ratios from the ITA18-NESS GMM [21] for three magnitude levels, $M_W = 5$ (left), $M_W = 6$ (center), and $M_W = 7$ (right), as a function of the Joyner-Boore distance $R = 5$ km, 15 and 30 km (top panels) and of site conditions $V_{S30} = 150$ m/s, 270 m/s, and 560 m/s (bottom panels). The average of the median V/H for different focal mechanisms is considered.

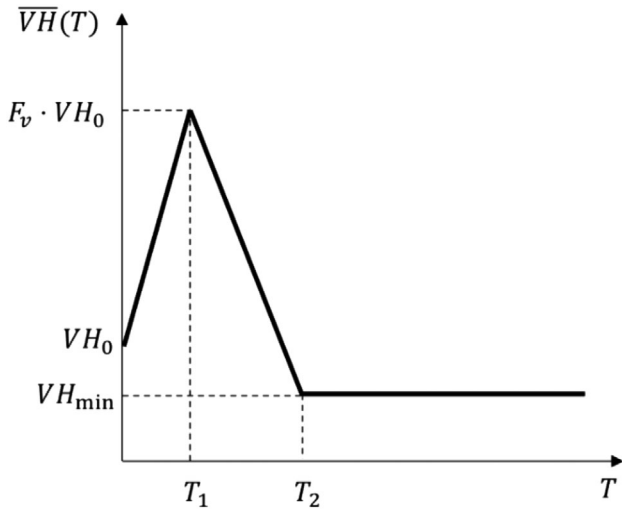


FIGURE 5 | The proposed V/H factor according to Equation (12).

affecting the V/H response spectral ratio and, at the same, manageable to be cast in a normative framework, the following functional form, as illustrated in Figure 5, is introduced:

$$\overline{VH}(T) = \begin{cases} VH_0 + \left(\frac{F_v - 1}{T_1}\right) \cdot VH_0 \cdot T & T \leq T_1 \\ F_v \cdot VH_0 - \left(\frac{F_v \cdot VH_0 - VH_{min}}{T_2 - T_1}\right) (T - T_1) & T_1 < T \leq T_2 \\ VH_{min} & T > T_2 \end{cases} \quad (12)$$

where:

- T_1 is the period corresponding to the peak of V/H;
- T_2 is the corner period defining the beginning of the long-period branch of V/H which is assumed to saturate to a constant value;
- VH_0 is the short-period value of V/H at $T = 0$, controlled by the vertical PGA;
- F_v is the maximum amplification factor of V/H ratio with respect to VH_0 governing the dynamically amplified short-period spectral plateau of the V spectrum;
- VH_{min} defines the value of the long-period constant branch of the V/H ratio at periods larger than T_2 .

It is worth noting that a similar effort to balance the accuracy from observational evidences with the simplicity required by normative applications, has guided the study by Kale and Akkar [39], who proposed an empirically-based formulation to develop the V design spectrum from the H one. In their expression, the V spectral ordinates are computed from the short-period and 1.0 s H response accelerations on reference rock as a function of the V_{S30} . Moreover, the decay of the V spectrum in the intermediate-to-long period range is captured more accurately through specific parameters empirically calibrated (namely, the upper corner period of the constant vertical acceleration plateau as well as the decay rate as a function of T).

In the following, the background for calibrating the parameters, T_1 , T_2 , VH_0 , F_v and VH_{min} , including their variability, is provided,

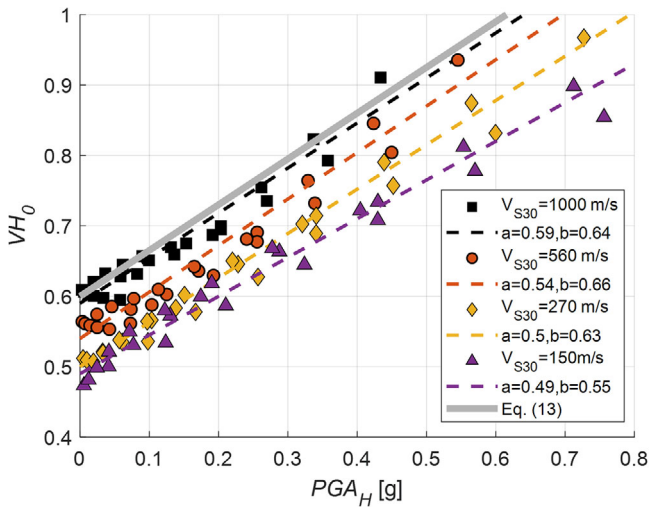


FIGURE 6 | Relationship between VH_0 and PGA_H (i.e., horizontal PGA) as a function of site conditions ($V_{S30} = 1000, 560, 270,$ and 150 m/s). For each site class, the scattered dots correspond to different scenario earthquakes with M_W in the range 4.7–7.2 and R in the range 5–50 km, while the dashed line represents the best-fitting least-squares linear regression with intercept a and slope b (the values are given in the legend). The thick gray line is the proposed relationship for VH_0 , with the parameters denoted by Equation (13). All plotted VH_0 values are averaged on the focal mechanism.

as a function of M_W , R and site class (the influence of the focal mechanism is neglected, given its marginal influence).

3.2.1 | Corner Periods: T_1 and T_2

As noted in Figure 4, the median V/H ratios from the ITA18-NESS GMM indicate that both the period T_1 corresponding to the peak value and the period T_2 corresponding to the start of the constant V/H branch, have a limited dependence on (M_W , R) and on site conditions. T_1 takes values typically around 0.05–0.07 s, while a limited variability of T_2 is found between around 0.15 and 0.30 s, with increasing values as M_W increases. It is worth noting that, unlike the functional form adopted in the ASCE 7–22 provisions (see Figure 1), the proposed V/H factor assumes, for simplicity, a single peak at 0.05 s, aiming at reducing the number of model parameters. However, a spectral plateau in a small interval around the period T_1 may be easily introduced for possible refinements.

3.2.2 | Short-Period V/H Ratio: VH_0

To express the dependency of VH_0 on the seismicity of the target site in a format suitable for normative use, its variability with respect to the horizontal peak ground acceleration (PGA_H) on rock conditions is analyzed, as shown in Figure 6. For this purpose, PGA_H is computed using the ITA18 GMM for the H components, while VH_0 , the latter being defined as the zero-period value of the V/H spectral ratio, is derived from the corresponding ITA18 GMM for V/H ratio. These predictions are evaluated for varying earthquake scenarios, with M_W in the range

TABLE 1 | Proposed values for F_v and VH_{min} as a function of the classification according to the EC8 site categories (representative values of V_{S30} are provided in brackets).

EC8 site class	F_v	VH_{min}
A ($V_{S30} = 1000$ m/s)	1.30	0.70
B ($V_{S30} = 560$ m/s)	1.40	0.55
C ($V_{S30} = 270$ m/s)	1.60	0.45
D-E ($V_{S30} = 150$ m/s)	1.75	0.35

4.2–7.2, R up to 50 km (averaged on focal mechanisms), and variable site conditions ($V_{S30} = 1000, 560, 270,$ and 150 m/s).

The results indicate that the variability of VH_0 with PGA_H can be expressed by the following linear relationship:

$$VH_0 = a + b \cdot PGA_H \quad \text{with} \quad a = 0.6, \quad b = 0.65 (PGA_H \text{ in g}) \quad (13)$$

Note that best-fitting a and b parameters of the linear regression vary slightly with site conditions, as shown in the legend of Figure 6. However, as a reasonable simplification, the dependence on site class is neglected and conservative values are assumed for both the intercept and slope, as indicated in Equation (13).

3.2.3 | Amplification Factor: F_v

The empirical V/H spectra from ITA18-NESS model suggest that the parameter F_v is poorly correlated with M_W , while it depends moderately on distance R and on site conditions. This is shown in Figure 7, where F_v , computed as the ratio between the peak V/H ratio and VH_0 , is plotted, on the left hand side, as a function of M_W , for a reference distance $R = 15$ km, and, on the right hand side, as a function of distance R for different soil classes (for the same site classes as considered previously). Larger values of F_v are found for decreasing soil stiffness (lower V_{S30}) and also for decreasing distance R , that is, for near-source scenarios, while the dependence on M_W can be considered negligible. The negligible dependence on M_W indicates that the source scaling of the vertical component is very similar to that of the horizontal both at short and long periods, as also discussed in Ramadan et al. [21]. Given that in the European and Italian context, seismic hazard is typically governed by local earthquakes, a reference distance $R = 15$ km is considered so that the F_v values depend solely on site conditions. Although not shown here for sake of brevity, the dependence of F_v on PGA_H is found to be very weak, especially in the range of peak accelerations of engineering interest (i.e., larger than 0.1 g approximately). The proposed values of F_v , as listed in Table 1 and displayed by the superimposed dash lines in Figure 7 (right panel), range between 1.3 and 1.75, going from rock (site class A) to soft soils (classes D–E), respectively.

3.2.4 | Long-Period V/H Ratio: VH_{min}

Figure 8 shows the trends of VH_{min} , computed from the V/H spectral ordinates averaged in the period range between 0.3 and 4 s, as a function of M_W and for a reference distance $R = 15$ km (left), and as a function of distance R for different soil classes

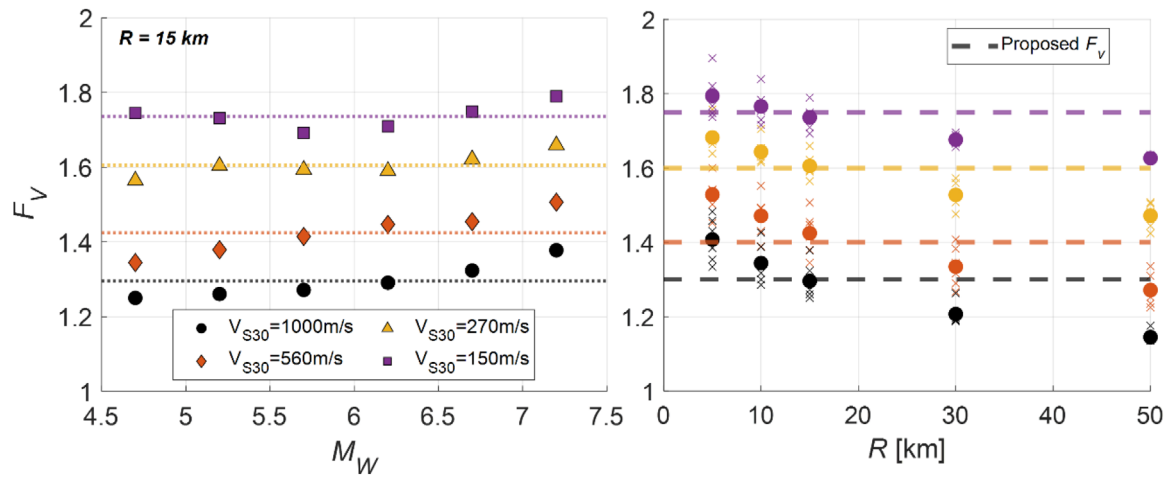


FIGURE 7 | Left: values of F_v as a function of M_W , for a reference distance $R = 15$ km, for different site classes ($V_{S30} = 1000, 560, 270$, and 150 m/s); the superimposed dotted lines represent the values averaged on M_W . Right: Values of F_v (crosses: values for each M_W , dots: average values on M_W) as a function of R , for the different soil classes; the superimposed dashed lines represent the proposed values of F_v (see Table 1). All plotted F_v values are averaged on the focal mechanisms.

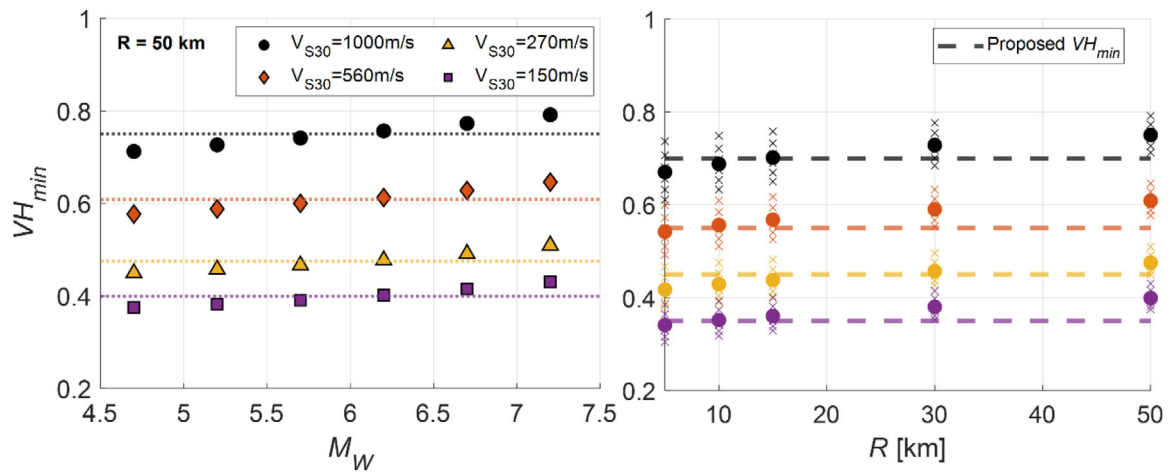


FIGURE 8 | Left: values of VH_{min} as a function of M_W , for a reference distance $R = 50$ km, for different soil classes ($V_{S30} = 1000, 560, 270$, and 150 m/s). The superimposed dotted lines represent the average values on M_W . Right: Values of VH_{min} (crosses: values for each M_W , dots: average values on M_W) as a function of R , for the different soil classes. The superimposed dashed lines represent the proposed values of VH_{min} (see Table 1). All plotted VH_{min} values are averaged on the focal mechanisms.

(right). VH_{min} turns out to be poorly dependent on the pair (M_W, R) , while a moderate correlation with site conditions is found. Similarly to F_v , given the limited dependence on M_W and R , also VH_{min} is found to be poorly correlated with PGA_H . Therefore, the proposed values of VH_{min} , as listed in Table 1 and displayed by the superimposed dashed lines in Figure 8 (right panel), account explicitly for the dependence on site conditions, ranging between 0.35 and 0.7 for soft soils (class D) and for rock (class A), respectively.

4 | V/H Ratios From PSHA

The proposed V/H factor of Equation (12) is given in a simpler format than the one of a GMM, because, instead of incorporating the basic explanatory variables typically used in an empirical predictive model, such as magnitude, source-to-site distance and

focal mechanism, it is defined solely as a function of PGA_H on reference rock conditions and of a site conditions proxy (i.e., V_{S30} or ground category). These parameters are commonly those adopted to define the seismic action within a normative framework. In spite of the simplicity of this format, the proposed V/H factor was found to reproduce reasonably well the main features of its dependence on distance, magnitude and site conditions. However, the agreement with the average V/H response spectral ratios obtained from records does not imply the agreement with the corresponding V/H ratio of the UHS obtained from a PSHA. Indeed, as well known, the UHS are the combined result of contributions from different earthquakes of different magnitude and distance. The result of such combination may be different when considering separately the UHS for the H and V components. As a consequence, the V/H ratio of UHS may be different from the average V/H ratio of records of specific earthquakes. However, based on the relatively poor dependence

on magnitude and distance of the parameters of Equation (12), as pointed out in the previous section, it may be argued that the V and H UHS may keep approximately the same spectral ratios as the corresponding ground motions. This may be especially true if, as in the case of most Italian and European sites, seismic hazard, at least at the standard values of return period (i.e., 475 years), is mostly governed by earthquakes within a limited range of magnitude and distance.

To check this argument, a simplified PSHA was carried out at four sites in Italy with different seismic hazard levels, namely L'Aquila (Abruzzi, Central Italy), Milano (Lombardia, Northern Italy), Gemona (Friuli, NorthEastern Italy), Potenza (Basilicata, Southern Italy). For this purpose, the area source model and the corresponding seismicity parameters of the Gutenberg-Richter relationship were taken from Visini et al. [40]. The software R-CRISIS [41] was used for the PSHA calculations.

For the H and V ground motion predictions we adopted the ITA18-based models, respectively, leveraging the full consistency between the two models. Results shown here are limited to the RP of 475 and 2475 years. For each test site and RP , PSHA are obtained on both rock ($V_{S30} = 800$ m/s) and soft site category ($V_{S30} = 270$ m/s).

The results of these PSHA are used to derive the V response spectrum using two approaches. In the first approach (A1), the V and H UHS have been obtained separately from the PSHA for a given RP , and the corresponding V/H ratios have been computed. As noted previously, the V and H UHS may be driven by different earthquake scenarios, so that the corresponding V/H ratio may be different from that provided by records. Such inconsistency may pose obstacles for some engineering applications, such as in the selection of hazard-consistent three-component ground motions to be used in dynamic time history analyses of structures. Indeed, as recalled from the previous survey, in the international norms it is generally preferred to consider the H spectrum as primary intensity measure and derive from that the V spectrum based on suitable V/H factors. As a second approach (A2), which is more consistent with the current normative framework, the V spectrum is obtained by scaling the H UHS. For this purpose, the median V/H ratio is computed, at a selected set of spectral periods from the ITA18-NESS GMM, using the magnitude and distance ($M_w(T)$, $R(T)$) derived from the hazard disaggregation of the H component. Although a rigorous solution would require a full vector-based hazard analysis [42], this approach corresponds to the conditional hazard approach, in which the H spectrum is the primary intensity measure and the V/H ratio is the secondary one.

The V/H ratios obtained from the previous approaches are shown in Figure 9, for the four sites under consideration (on reference rock category) and for the two RP s (left: 475 years, right: 2475 years). As a reference, these ratios are compared in Figure 9 with:

1. the ratio of V and H elastic design spectrum according to the current Italian seismic norm NTC18 using, for each site and RP , the base hazard parameters as prescribed by NTC18; note that, in terms of definition of V spectra, NTC18 closely reproduces the EC8 regulation currently in force [43];

2. same as point 1), but according to the EC8-1-1 criteria, using the spectral parameters $S_{\alpha,RP}$ and $S_{\beta,RP}$ corresponding to the H NTC18 design spectrum and Equations (6)–(11) for the V design spectrum;
3. the V/H factor of Equation (12), where $T_2 = 0.2$ s is adopted for all sites, although, as commented previously, a larger value (say 0.3 s) may be more suitable for high seismicity sites, such as L'Aquila and Gemona, and a smaller one (say 0.15 s) may be suitable for low seismicity, such as Milano.

The effect of site conditions on the V/H ratios is investigated in Figure 10, where, for two sites, namely L'Aquila (top) and Milano (bottom), for $RP = 475$ years, the same comparison as in Figure 9 is shown but for both generic rock with $V_{S30} = 1000$ m/s (left) and soft site with $V_{S30} = 270$ m/s (right). In order to extend the comparison to the international normative context, besides NTC18 and EC8-1-1, the ASCE 7-22 design V/H ratios are also included, using input parameters set in order to provide consistency of the design spectral ordinates for the H component. For the comparison on soft soils, consistency on the H design spectrum is still assured and site effects on V spectrum are taken into account by following the criteria prescribed in each seismic norm for the corresponding ground category and, with reference to the V/H factor of Equation (12), using the site-dependent parameters in Table 1.

These comparisons point out that:

- results of the A1 and A2 hazard-based approaches are very similar, as justified by the consistency of disaggregation results for the V and H components for the different sites considered, where, as noted previously, hazard is dominated by earthquakes in a small interval of magnitude and distance. Some relatively minor discrepancies are observed at short periods in the case of L'Aquila, with hazard mostly contributed by large magnitude and short distance earthquakes, in a range where the empirical V/H ratios have the largest variability;
- the proposed V/H formulation of Equation (12) and the V/H ratios from the hazard-based A1 and A2 approaches are in reasonably good agreement, regardless of the hazard levels, of the RP and of the site conditions (rock vs. soft), thus supporting the argument that, in the Italian and European context, it is reasonable to obtain the V design spectrum by scaling the H spectrum by a simplified V/H factor;
- a good agreement is also found with the V/H ratios resulting from the EC8-1-1, although there is a tendency of overestimation in the intermediate period range, between 0.1 and 0.3 s approximately;
- the comparison of the proposed V/H ratios with ASCE 7-22 is also satisfactory in spite of the very different geographic contexts;
- while in reasonable agreement for short periods (up to 0.2 s) and for moderate-to-high seismicity sites, the NTC18 design ratios tend to deviate from both the V/H ratios of UHS and from Equation (12), providing values of the spectral ratios significantly lower in the intermediate to long period range and for soft site conditions (see Figure 10, right, and discussion at following point). For low seismicity sites, such as Milano,

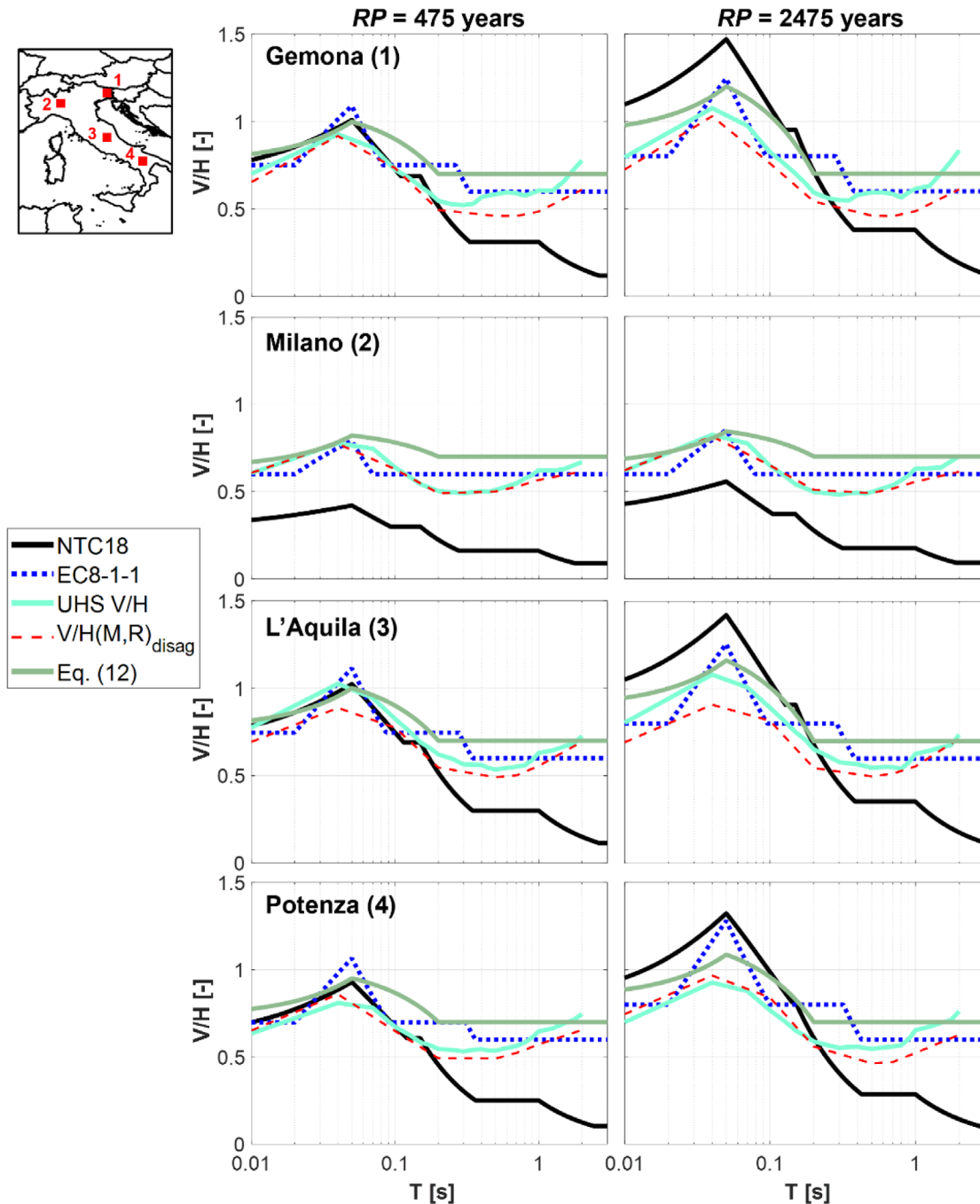


FIGURE 9 | Comparison of the V/H factor of Equation (12) at the four test sites (1: Gemona, 2: Milano, 3: L'Aquila, 4: Potenza, see location on the top left map), on outcropping rock conditions, for return periods $RP = 475$ years (left) and $RP = 2475$ years (right), with the V/H ratios from PSHA obtained following the A1 and A2 approaches introduced in the text and with the code-based V/H ratios from both NTC18 and EC8-1-1. For Equation (12), $T_2 = 0.2$ s is assumed.

the NTC18 V/H ratios underestimate significantly the A1 and A2 hazard-based ratios in a broad period range;

- as regards the dependence of V seismic action on site conditions, it should be noted that, while site conditions enter directly in the functional form of the V/H ratio according to Equation (12), as well as according to ASCE 7–22, for both NTC18 and EC8-1-1 the V/H ratio are modulated by the H spectral ordinates alone, therefore providing an indirect dependence on site conditions.

5 | Conclusions

In this paper, we have presented the background studies related to the definition of the vertical seismic action in view of the next generation seismic norms in the European and Italian context. To this end, we have reviewed the V spectra for design in the EC8-1-1 for which, for ease-of-use, a simple regularized form was adopted. In these formulations, the $f_{vh\alpha}$ and $f_{vh\beta}$ factors, representing the V/H ratio at the short period spectral plateau and at $T = 1$

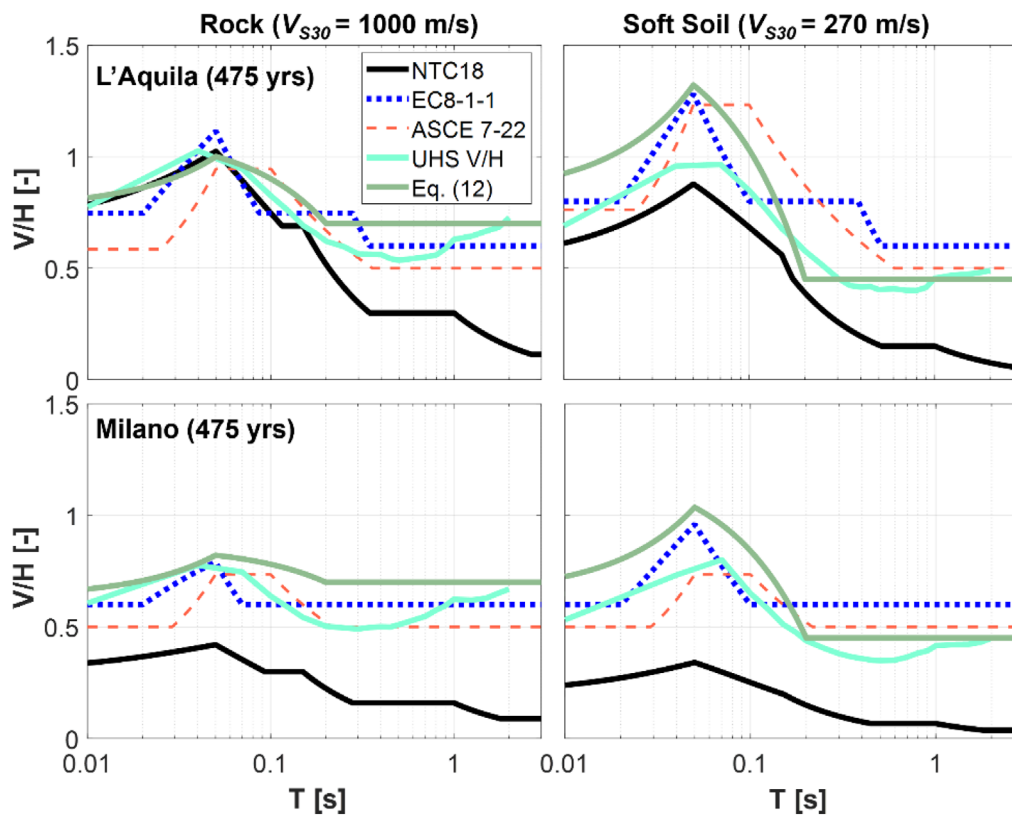


FIGURE 10 | Comparison of Equation (12) with the V/H ratios of UHS (A1 approach) as well as with the V/H ratios from both NTC18, EC8-1-1 and ASCE 7-22 design spectra, at L'Aquila (top) and Milano (bottom), for $RP = 475$ years, for generic outcropping rock with $V_{S30} = 1000$ m/s (left) and soft soil with $V_{S30} = 270$ m/s (right).

s, respectively, are independent on site conditions, while they depend only on the seismicity level in terms of $f_{vh\alpha}$ according to Equation (10). An indirect dependency of the resulting V/H ratio on site conditions is related to the site-dependence of the design H spectral parameters, S_α and S_β , according to Equations (6) and (7).

A more detailed alternative to the EC8-1-1 formulation was explored, by the introduction of a simplified V/H factor that, with a similar aim as in the ASCE 7-22, includes an explicit dependence on the seismicity level (i.e., PGA_H) and on the site class. The rationale behind this proposal is to express the V/H spectral ratios as a function of relatively few hazard parameters, in a format suitable for potential implementation within a normative framework, being, at the same time, capable of capturing the variability of the V/H ratios with the main physical factors (magnitude, distance, and site effects), as found in existing empirical studies.

The hazard consistency of the proposed V/H factor has been tested at some example sites in Italy, representative of both low and high seismicity regions, through a comparison with the hazard-based V/H ratios obtained considering, on one side, the ratios of the H and V UHS obtained by two separate PSHA for the corresponding ground motion components and, on the other side, the median V/H ratios from the reference GMM using the period-dependent magnitude and distance scenarios from the disaggregation of the H hazard. The comparison has been extended to include the code-based V/H ratios from the

EC8-1-1 vertical design spectra, from the Italian norms NTC18. Results from ASCE 7-22 have also been included for reference. It was found that the proposed V/H factor provides results in reasonably good agreement with the V/H ratios from PSHA, regardless of the seismicity conditions, of the return period and of site conditions (rock vs. soft), being able to capture the main features (peak values and decay with period) of the probabilistic results. Such agreement can be explained because of the slight dependence of the V/H response spectral ratio on magnitude and distance, at least in the range of local earthquakes, typically with small-to-moderate magnitude, that dominate hazard in Italy and Europe.

A similar positive performance is also obtained both by using the EC8-1-1 prescriptions, although the resulting V spectra tend to be slightly overconservative especially for soft site conditions in the intermediate (0.1–0.5 s) period range, and by using ASCE 7-22, in spite of the different seismotectonic context. On the other hand, NTC18 tends to underestimate the V/H ratios of UHS, especially in the intermediate to long range of vibration periods and for softer sites, posing potential issues in the definition of the seismic action for design, such as for the selection of three-component spectrum-compatible ground motion time series for non-linear dynamic analyses of structures.

It can be concluded that, although inspired by an ease-of-use motivation that suggested to avoid the direct dependence of the V spectral parameters on site conditions, the formulation of vertical design spectra according to the EC8-1-1 provides reasonably good

results for both rock and soft soils. Introducing a dependency of the V spectral parameters on site conditions, as adopted in the ASCE 7–22 as well as considered in the factor of Equation (12), provides a slight improvement, at the price of a slight increase of complexity in the formulation.

Acknowledgments

This study has been conducted within the research programs ReLUIIS (Rete dei Laboratori Universitari di Ingegneria Sismica) in the framework of Dipartimento della Protezione Civile (DPC)-ReLUIIS Agreements 2022–2023 and 2024–2026 “Input sismico, normativa e microzonazione” WP18, funded by the Presidenza del Consiglio dei Ministri—DPC, Italy. The authors are grateful to Francesca Pacor and Giovanni Lanzano for their fruitful discussions during the development of this work and to Arsalan Bazrafshan for this help to construct the tripartite plots of the EC8-1-1 design spectra. The proposal for the V spectra in the EC8-1-1 was developed while the second author (RP) was member of the project team PT1, in charge of drafting Part 1 of the revised Eurocode 8. Discussions and contributions by the other members of PT1, namely, P. Labbé, A. Benavent, M. Dolsek, J. Schwarz, T. Wenk, and by the SC8 chairman P. Bisch are gratefully acknowledged. Authors are grateful to the two anonymous reviewers and to the Associate Editor, Iunio Iervolino, for their constructive comments that helped improving the paper. One of these pointed out the explanation of the 0.2 factor in the combination rule of the V component in ASCE 7–22.

Data Availability Statement

Data sharing not applicable to this article as no datasets were generated or analyzed during the current study.

References

1. J. Dewey and P. Beyerly, “The Early History of Seismometry (to 1900),” *Bulletin of Seismological Society of America* 59, no. 1 (1969): 183–227.
2. A. G. Brady, “Strong-Motion Accelerographs: Early History,” *Earthquake Engineering and Structural Dynamics* 38, no. 9 (2009): 1121–1134, <https://doi.org/10.1002/eqe.913>.
3. M. D. Trifunac and M. I. Todorovska, “Evolution of Accelerographs, Data Processing, Strong Motion Arrays and Amplitude and Spatial Resolution in Recording Strong Earthquake Motion,” *Soil Dynamics and Earthquake Engineering* 21, no. 6 (2001): 537–555, [https://doi.org/10.1016/S0267-7261\(01\)00013-6](https://doi.org/10.1016/S0267-7261(01)00013-6).
4. F. Penta, “Alcuni Provvedimenti Presi Dopo i Grandi Terremoti Italiani Dei Secoli XVIII, XIX e XX,” *Rivista Italiana Di Geotecnica* (1963).
5. A. Danusso. La statica delle costruzioni antisismiche. *Atti della Società degli Ingegneri e Architetti di Torino* (1909) Anno XLIII; 65–87.
6. M. A. Biot, “Theory of Elastic Systems Vibration Under Transient Impulse With an Application to Earthquake-Proof Buildings,” *Proceedings of the National Academy of Sciences* 19, no. 2 (1933): 262–268, <https://doi.org/10.1073/pnas.19.2.262>.
7. G. W. Housner, “Spectrum Intensity of Strong Motion Earthquakes,” in *Proceedings of the Symposium on Earthquakes and Blast Effects on Structures*, Earthquake Engineering Research Institute (1952), 20–36.
8. N. M. Newmark and W. J. Hall, *Earthquake Spectra and Design* (Earthquake Engineering Research, 1982).
9. N. N. Ambraseys and J. Douglas, “Near-Field Horizontal and Vertical Earthquake Ground Motions,” *Soil Dynamics and Earthquake Engineering* 23 (2003): 1–18, [https://doi.org/10.1016/S0267-7261\(02\)00153-7](https://doi.org/10.1016/S0267-7261(02)00153-7).
10. ASCE/SEI 7–22. *Minimum Design Loads and Associated Criteria for Buildings and Other Structures* (American Society of Civil Engineering (ASCE), 2022).
11. E. Rosenblueth and H. Contreras, “Approximate Design for Multicomponent Earthquakes,” *Journal of Engineering Mechanics ASCE* 103 (1977): 895–911.
12. CEN/TC 250/SC 8. Eurocode 8, Earthquake Resistance Design of Structures—Part 1–1: General Rules and Seismic Action. FprEN 1998-1-1:2024 (2024).
13. CEN/TC 250/SC 8. Eurocode 8, Earthquake Resistance Design of Structures—Part 5: Geotechnical Aspects, Foundations, Retaining and Underground Structures. FprEN 1998-5:2024 (2024).
14. Y. Bozorgnia and K. W. Campbell, “The Vertical-to-Horizontal Response Spectral Ratio and Tentative Procedures for Developing Simplified V/H and Vertical Design Spectra,” *Journal of Earthquake Engineering* 8 (2004): 175–207, <https://doi.org/10.1080/13632460409350486>.
15. Y. Bozorgnia and K. W. Campbell, “Ground Motion Model for the Vertical-to-Horizontal (V/H) Ratios of PGA, PGV, and Response Spectra,” *Earthquake Spectra* 32, no. 2 (2016): 951–978, <https://doi.org/10.1193/100614eqs151m>.
16. Y. Bozorgnia and K. W. Campbell, “Vertical Ground Motion Model for PGA, PGV, and Linear Response Spectra Using the NGA-West2 Database,” *Earthquake Spectra* 32, no. 2 (2019): 979–1004, <https://doi.org/10.1193/072814eqs121m>.
17. S. Akkar, M. A. Sandikkaya, and B. O. Ay, “Compatible Ground-Motion Prediction Equations for Damping Scaling Factors and Vertical-to-Horizontal Spectral Amplitude Ratios for the Broader Europe Region,” *Bulletin of Earthquake Engineering* 12 (2014): 517–547, <https://doi.org/10.1007/s10518-013-9537-1>.
18. Z. Çağnan, S. Akkar, O. Kale, and A. Sandikkaya, “A Model for Predicting Vertical Component Peak Ground Acceleration (PGA), Peak Ground Velocity (PGV), and 5% Damped Pseudospectral Acceleration (PSA) for Europe and the Middle East,” *Bulletin of Earthquake Engineering* 15 (2017): 2617–2643.
19. Z. Gülerce, R. Kamai, N. A. Abrahamson, and W. J. Silva, “Ground Motion Prediction Equations for the Vertical Ground Motion Component Based on the NGA-W2 Database,” *Earthquake Spectra* 33, no. 2 (2017): 499–528, <https://doi.org/10.1193/121814EQS213M>.
20. J. P. Stewart, D. M. Boore, E. Seyhan, and G. M. Atkinson, “NGA-West2 Equations for Predicting Vertical-Component PGA, PGV, and 5%-Damped PSA From Shallow Crustal Earthquakes,” *Earthquake Spectra* 32 (2016): 1005–1031, <https://doi.org/10.1193/072114eqs116m>.
21. F. Ramadan, C. Smerzini, G. Lanzano, and F. Pacor, “An Empirical Model for the Vertical-to-Horizontal Spectral Ratios for Italy,” *Earthquake Engineering and Structural Dynamics* 50 (2021): 4121–4141, <https://doi.org/10.1002/eqe.3548>.
22. DZ TS 1170.5:2024. New Zealand Technical Specification Structural Design Actions. Part 5: Earthquake Actions—New Zealand; 2024. Public Consultation Draft.
23. P. K. Malhotra, *Site-Specific Ground Motions for Seismic Design of Buildings and Other Structures* (ASCE Press, 2022), <https://doi.org/10.1061/9780784415962>.
24. P. Labbé and R. Paolucci, “Developments Relating to Seismic Action in the Eurocode 8 of Next Generation,” in *ECEES 2022*, eds. R. Vacareanu and C. Ionescu (Springer Proceedings in Earth and Environmental Sciences, 2022), 26–46, https://doi.org/10.1007/978-3-031-15104-0_2.
25. ASCE/SEI 7–16. *Minimum Design Loads for Buildings and Other Structures* American Society of Civil Engineering (ASCE) (2016).
26. National Earthquake Hazards Reduction Program—NEHRP. *Recommended Seismic Provisions for New Buildings and Other Structures (FEMA P-20821)* (Building Seismic Safety Council, 2020).
27. CS.LL.PP.—Consiglio Superiore dei Lavori Pubblici. *Norme Tecniche delle Costruzioni*, DM 17 gennaio 2018, Gazzetta Ufficiale della Repubblica Italiana 42 (2018).
28. Turkish Building Earthquake Code TBEC18. *Regulations for Buildings to be Constructed in Earthquake Prone Areas*, Ankara, Turkey (2018).

29. CED 39/T-10. Draft Indian Standard Criteria for Earthquake Resistant Design of Structures Part 1 General Provisions. Seventh Revision of IS 1893 (Part 1) (2023).
30. L. Danciu, D. Giardini, G. Weatherill, et al., “The 2020 European Seismic Hazard Model: Overview and Results,” preprint, *EGU Sphere* 36 (2024), <https://doi.org/10.5194/egusphere-2023-3062>.
31. R. Paolucci, M. Aimar, A. Ciancimino, et al., “Checking the Site Categorization Criteria and Amplification Factors of the 2021 Draft of Eurocode 8 Part 1–1,” *Bulletin of Earthquake Engineering* 19 (2021): 4199–4234, <https://doi.org/10.1007/s10518-021-01118-9>.
32. G. Lanzano, L. Luzi, F. Pacor, et al., “A Revised Ground-Motion Prediction Model for Shallow Crustal Earthquakes in Italy,” *Bulletin of the Seismological Society of America* 109, no. 2 (2019): 525–540, <https://doi.org/10.1785/0120180210>.
33. F. Pacor, C. Felicetta, G. Lanzano, et al., “NESS1: A Worldwide Collection of Strong-Motion Data to Investigate Near-Source Effects,” *Seismological Research Letters* 89, no. 6 (2018): 2299–2313, <https://doi.org/10.1785/0220180149>.
34. S. Sgobba, C. Felicetta, G. Lanzano, F. Ramadan, M. D’Amico, and F. Pacor, “NESS2.0: An Updated Version of the Worldwide Dataset for Calibrating and Adjusting Ground-Motion Models in Near-Source,” *Bulletin of the Seismological Society of America* 111, no. 5 (2021): 2358–2378, <https://doi.org/10.1785/01202100802021>.
35. R. Paolucci, F. Pacor, R. Puglia, G. Ameri, C. Cauzzi, and M. Massa, “Record Processing in ITACA, the New Italian Strong-Motion Database,” in *Earthquake Data in Engineering Seismology, Geotechnical, Geological and Earthquake Engineering Series*, eds. S. Akkar, P. Gulkan, and T. Van Eck (Springer, 2011), 79, 99–113, https://doi.org/10.1007/978-94-007-0152-6_8.
36. N. A. Abrahamson and J. J. Litehiser, “Attenuation of Vertical Peak Acceleration,” *Bulletin of the Seismological Society of America* 79, no. 3 (1989): 549–580.
37. K. W. Campbell, “Empirical Near-Source Attenuation Relationships for Horizontal and Vertical Components of Peak Ground Acceleration, Peak Ground Velocity, and Pseudo-Absolute Acceleration Response Spectra,” *Seismological Research Letters* 68, no. 1 (1997): 154–179, <https://doi.org/10.1785/gssrl.68.1.154>.
38. Z. Gülerce and N. A. Abrahamson, “Site-Specific Design Spectra for Vertical Ground Motion,” *Earthquake Spectra* 27, no. 4 (2011): 1023–1047.
39. Ö. Kale and S. Akkar, “A New Formulation for a Code-Based Vertical Design Spectrum,” *Earthquake Engineering and Structural Dynamics* 49, no. 10 (2020): 963–980, <https://doi.org/10.1002/eqe.3272>.
40. F. Visini, C. Meletti, A. Rovida, V. D’Amico, B. Pace, and S. Pondrelli, “An Updated Area-Source Seismogenic Model (MA4) for Seismic Hazard of Italy,” *Natural Hazards and Earth System Sciences* 22, no. 8 (2022): 2807–2827, <https://doi.org/10.5194/nhess-22-2807-2022>.
41. M. Ordaz, M. A. Salgado-Gálvez, and S. Giraldo, “R-CRISIS: 35 Years of Continuous Developments and Improvements for Probabilistic Seismic Hazard Analysis,” *Bulletin of Earthquake Engineering* 19, no. 7 (2021): 2797–2816, <https://doi.org/10.1007/s10518-021-01098-w>.
42. P. Bazzurro and C. A. Cornell, “Vector-Valued Probabilistic Seismic Hazard Analysis,” *Seismological Research Letters* 72, no. 2 (2001): 273.
43. CEN—European Committee for Standardization Eurocode 8. Design of Structures for Earthquake Resistance—Part 1: General Rules, Seismic Actions and Rules for Buildings, EN 1998-1 (2004).